INTERNATIONAL JOURNAL of RENEWABLE ENERGY RESEARCH
S. K. Gurijala and J. P. Darsy., Vol.16, No.1, March, 2026

An Investigation on Efficient Controller Tuning Methods for Controlling Dual Input Single Output Buck Converter used for Electric Vehicle Application

Sarala Kumari Gurijala*, John Pradeep Darsy*‡

*School of Electronics Engineering, VIT-AP University, Amaravati, 522237, India.

(gurijalasaralakumari@gmail.com, johnpradeepdarsy@gmail.com)

‡ Corresponding Author: John Pradeep D, School of Electronics Engineering, VIT-AP University, Amaravati, 522237, India.

Tel: +91 9566810027, johnpradeepdarsy@gmail.com

Received: 19.12.2023 Accepted:10.03.2024

Abstract- Multiport DC–DC converters play an important role in energy conversion and integration in renewable energy source (RES) systems and electric vehicles. In multi-source environments, conventional buck converters cannot combine voltages, and using separate converters for each source is uneconomical. To address this limitation, researchers have developed multiport converter topologies. This work investigates a Dual-Input Single-Output (DISO) buck converter with the PID controllers in the feedback loop. There are a variety of tuning techniques available for tuning the gain parameters. Among them, two PID tuning approaches are considered: response-based methods and transfer-function-based methods. The response-based approach is further classified into Open Loop Transient Response (OLTR) methods and Error Performance Index (EPI) methods. The PID gains for both voltage and current controllers are obtained using these tuning techniques, and their performance is evaluated using time-domain and frequency-domain parameters. Results show that the IAE-2 PID tuning method provides the best performance for the voltage controller, with an 81% difference in peak overshoot between the best and worst tuning methods. For the current controller, the Min-IAE-Wang and Min-ITAE-Wang methods perform best. Although the peak overshoot variation is only 1.2%, a significant difference of 176^0 in phase margin is observed. The analysis is carried out using MATLAB/Simulink.

Keywords DC-DC converter, dual input single output (DISO), PID controller; open loop transient response (OLTR); and error performance indexed (EPI).

1. Introduction

The use of renewable energy sources in power generation has picked up recently, thereby promoting clean and green energy. This also necessitates the development and utilization of various power converters to enable the conversion of power from DC to DC, DC to AC, and vice-versa. RES are intermittent in nature, so voltage fluctuations are quite common. Despite of fluctuations, to maintain constant output, these power converters are very useful. Generally, the nature of the current harvested from RES is DC in nature, so there is a requirement for effective DC-DC converters [1].

Conventional DC-DC converter topologies like buck, boost, and buck-boost are improvised by the researchers to achieve more efficiency in the conversion process and to decrease the stress on power electronic switches. Multi-Input Multi-Output (MIMO), and Multi-Input Single-Output (MISO) converters [2,3] are introduced to facilitate the integration of different RES and to reduce the count of converters. These converters have the provision to integrate more than one source at its input and provide a single output or more based on the topology and requirement of the consumer. This present work discusses about a Dual Input Single Output (DISO) buck converter with an application to electric vehicles. DISO converter belongs to the family of multi-input single-output converters and it utilizes two input sources and provides single output. Such types of converters are used in hybrid electric vehicles [4], microgrids, Low/High power solar PV systems [5], DC distribution systems, and

military equipment [6] to name a few. These converters integrate more than one source having different characteristics and combine the advantages of both sources, such that the efficiency and reliability of the converter are improved. In case of integrating two or more RES sources, more than one DC-DC converter is required and to integrate various sources, a DC bus is inevitable. The multi-input converter can reduce the number of converters and also helps in eliminating the use of DC bus [7]. A multiphase interleaved bidirectional converter is used for the EV application in [8]. The nomenclature used in this work is given in Table 1.

Table 1. The abbreviations and their expansion used in present work

Abbreviation	Expansion
RES	Renewable Energy Sources
DISO	Double Input Single Output
PID	Proportional Integral and Derivative
MIMO	Multi Input Multi Output
EVs	Electric Vehicles
PHEVs	Plug-in Hybrid EVs
FCEVs	Fuel Cell EVs
BEVs	Battery-electric Vehicles
HEVs	Hybrid EVs
FC	Fuel Cell
OLTR	Open Loop Transient Response
CHR	Chien-Hrones-Reswick
CC	Cohen-Coon
EPI	Error Performance Index
PV	Photo Voltaic
ISE	Integral Square Error
ISTE	Integral Square Time Error
ISTSE	Integral Square Time Square Error
ITAE	Integral Time Absolute Error
ZN1	Ziegler-Nichols - 1
WJC	Wang-Jang-Chan
FOPID	Fractional Order PID
T_p	Peak Time
T_r	Rise Time
T_s	Settling Time
%OS	Percentage Overshoot

Although the power electronic converters are advantageous, they require a controller to provide a controlled or regulated output and also for reliable operation. Traditionally a PID controller is used in many of the applications as it is flexible, easy to implement, and industrial friendly. The PI and PID controllers are designed using the ZN tuning method for the buck converter to control the battery charging [9], to charge the E-scooters PV system, the boost converter is controlled by PI controller [10]. A dc-dc buck converter is controlled for Digital Peak current mode to verify the robustness using a PID controller [11]. Tuning a PID controller is an important task as the controller performance is completely dependent on the controller gain parameters. Different methods are available for tuning the PID controller gain parameters and all the tuning methods are not suitable for all applications. And one cannot say which tuning method is suitable for an application without proper analysis.

A dual input high step-up converter with a reduced number of switches is designed and analysed [12]. A PID controller design for a 3-input 2-output MIMO boost converter is presented in [13]. A single loop PID control for a Cuk converter is proposed and tested with various tuning methods with the conclusion that ITAE tuning methods perform better than other PID tuning methods [14]. OLTR and EPI tuning methods were tested on a PID controller to control the output temperature of the heat exchanger [15], and concluded that both the tuning methods provide satisfactory control. PI controller for a liquid level system [16], was designed using OLTR and EPI tuning methods for a faster response. A PID controller was designed to have control over the temperature in the heat exchanger with EPI tuning methods and finalized that the ITAE method provide better performance [17]. The PI and PID controllers were designed for a buck-boost converter with the transfer function based [18] tuning algorithms and it is concluded that the ITAE method performed better. And the PID controller tuning methods for applications such as aircraft cabin temperature control [19], for Wind turbine systems [20], for industrial heating furnace temperature control [22] are implemented.

In [21], a single closed loop control was implemented for a dual input single output DC-DC converter (DISO) with a PID and Fractional Order PID (FOPID) controller. It was concluded that the FOPID controller provides a stable output compared to a traditional PID controller. A Fuzzy PID control for the same application was implemented in [22]. These advanced controllers are computationally extensive even though they provide good control. The classical PID controller on the other hand can also provide good control with less computational burden, and design flexibility if they are properly investigated for better tuning methods. The present work provides a complete analysis of the PID controller tuning methods for a DISO converter. This is done using two closed-loop PI/PID controllers for the DISO converter.

Recently, a new configuration of DISO converters was proposed [23], in which integration of renewable energy sources was highlighted. In [24], a modified DISO Bidirectional SEPIC converter is proposed for Light EV applications. Another type of DISO converter is described for high reliability applications in [25] and studies the fault

tolerance of the switches. They have used the PID controller for a closed-loop control of the converter. A DISO converter with a coupled inductor having a high gain converter is proposed in [26], a PI controller was used for the controlling scheme but there is no mention of tuning methods and design of the controller. Some researchers designed the PID controller for the chopper to control the speed of a DC machine [27], Automatic load frequency control [28], and Automatic voltage regulator [29], using several tuning methods such as OLTR, EPI, etc.,

Tuning methods or algorithms play a vital role in designing a classical PID controller, to find the appropriate gain parameters which in turn are crucial for the functioning of the converter. However, no work was reported on the design of the PI/PID controller, analyzing different tuning methods for the selected DISO converter configuration. It is essential to analyze the tuning methods of a PID controller applied to a DISO converter as the PID controller is easy to use and is widely used in the control of switching circuits. The present work deals with probing the DISO converter with a PID controller with response-based tuning methods and transfer function based tuning methods [30], to control the voltage and current of the converter.

The organization of the manuscript is as follows: Section 1 deals with the introduction and literature review. Section 2 elucidates the Model of the converter. The implementation of the PID controller with tuning algorithms & tuning methods for both current control and voltage control is presented in section 3. The computation of the time domain and frequency domain performance indices are presented in section 4. In section 5, the summary of the results is presented. The conclusion of the work along with the analysis of the results is presented in section 6, followed by the references in section 7.

2. Model of the Converter

The Electric Vehicles (EVs) are categorized as 4 types. Battery-based Electric Vehicles (BEVs), Hybrid EVs (HEVs), Plug-in Hybrid EVs (PHEVs), and Fuel Cell EVs (FCEVs). The BEVs are comprised of rechargeable battery packs and produce zero emissions. The HEVs and PHEVs have internal combustion engines and produce harmful gases. The BEVs and PHEVs depend on the electricity to get charged, which burdens the power grid. FCEVs on the other hand are independent of the power grid and are eco-friendly but constrained by the cost of fuel used [31]. A grid-independent powertrain architecture using the advantage of DISO converter is shown in Fig.1. DISO buck converter integrates the power generated by fuel cells and PV. This eliminates the use of multiple dc/dc converters and effectively deals with integrating power generated from both sources to generate a constant voltage of 12 V. Different converters are also used for harvesting power from PV to charge EVs [32]. This voltage is used as a supply to auxiliary units such as the dashboard display, the powering of sensors, and other important electronic circuits in the EV. The induction motor used to drive the transmission is powered by an inverter which is fed through a boost converter and the input to this boost converter is derived from the output of the DISO converter. The circuit diagram of a dual input single output (DISO) buck converter is shown in Fig.2. The DISO converter is fed from two voltage sources with different magnitudes, two power switches, two diodes, an inductor, and a capacitor [33]. Based on the way switches S_1 and S_2 are switched ON and OFF, the converter could operate in 4 different modes. Different modes of operation of the converter are given in Table 2.

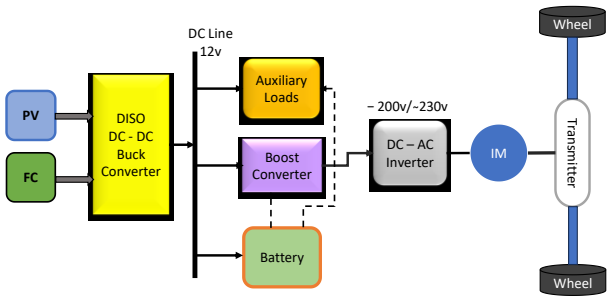

Fig. 1. Schematic of an EV with DISO converter.

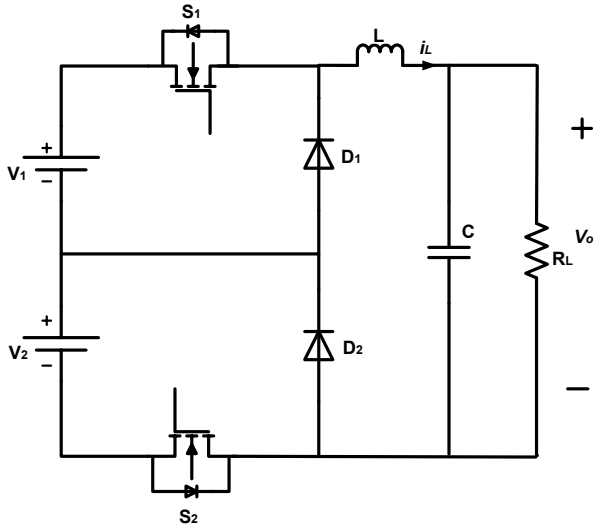

Fig. 2. DISO Buck converter circuit diagram.

Table 2. Relation between the condition of the switches and the mode of operation

Mode	S_1	S_2	Inference
I	ON	ON	$V_o = V_1 + V_2$
II	ON	OFF	$V_o = V_1$
III	OFF	ON	$V_o = V_2$
IV	OFF	OFF	$V_0 = 0$ V

Assuming $V_1 > V_2$ and $V_O > V_2$, the converter operates at a condition of $d_1 < d_2$ where d_1 and d_2 are the duty cycles of the gate driving circuits of power switches S_1 and S_2 respectively. In this case, the voltage source V_2 is considered as a primary source, this results in the converter operating in modes I, III, and IV. The schematic of the converter operating in modes I, III, and IV are shown in Fig.3.

In mode I, the two switches are ON, and the diodes are open-circuited. This results in current flowing through the inductor to the load and thus resulting in output voltage which

is the sum of two voltage sources. This condition is shown in Fig.3(a). The differential equations governing the two state variables i_L and v_C are given in Eq. (2) and (4).

$$V_L = -V_C + V_2 + V_1 \quad (1)$$

$$\frac{di_L}{dt} = \frac{1}{L}(-V_C + V_2 + V_1) \quad (2)$$

$$i_C = i_L - i_o \quad (3)$$

$$\frac{dv_C}{dt} = \frac{1}{C}\left(i_L - \frac{V_C}{R_L}\right) \quad (4)$$

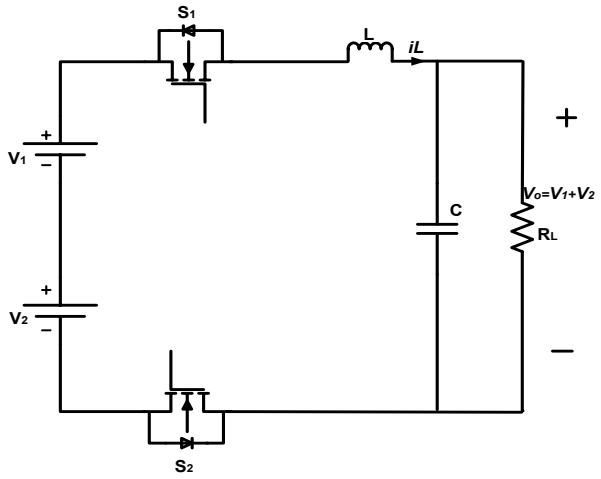

Fig. 3(a). Schematic of DISO converter operation in Mode-I.

In mode-III, Whenever switch S_1 is turned OFF and S_2 is turned ON, diode D_1 is in conduction mode and the current from source V_2 flows through the diode and inductor. The inductor current and capacitor voltage relations for the converter operating in mode-III are given using Eq. (5) and Eq. (6).

$$\frac{di_L}{dt} = \frac{1}{L}(V_2 - V_C) \quad (5)$$

$$\frac{dv_C}{dt} = \frac{1}{C}\left(i_L - \frac{V_C}{R_L}\right) \quad (6)$$

In mode IV, both the switches are turned OFF and the energy stored in the inductor is discharged through the load by turning the diodes D_1 and D_2 ON. The relations for inductor current and capacitor voltage for the DISO converter operating in mode-IV are given in Eq. (7) and Eq. (8).

$$\frac{di_L}{dt} = \frac{1}{L}(-V_C) \quad (7)$$

$$\frac{dv_C}{dt} = \frac{1}{C}\left(i_L - \frac{V_C}{R_L}\right) \quad (8)$$

From each of the modes of operation, the state-space matrices, of the converter are derived. The state variables for these matrices are the characteristics of energy storage elements used in the converter, which are the inductor current and capacitor voltage.

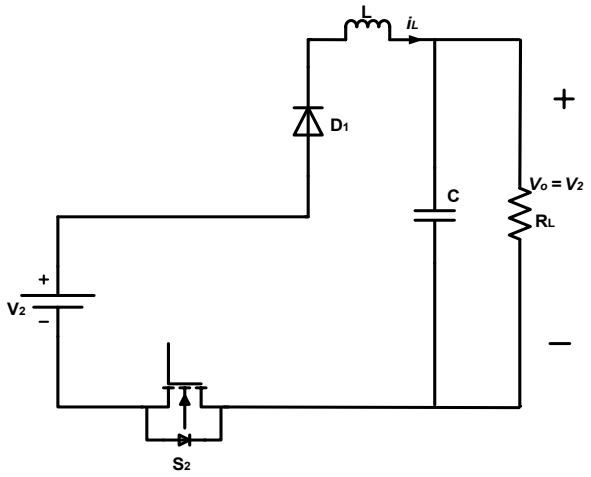

Fig. 3(b). Schematic of DISO converter operation in Mode-III.

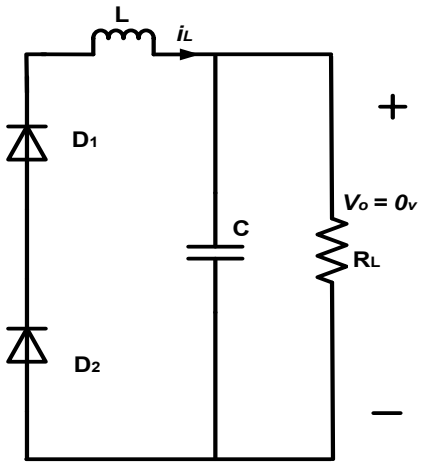

Fig. 3(c). Schematic of DISO converter operation in Mode-IV.

2.1. State Space Averaging Model

The acquired State space matrices from 3 operating modes are combined by multiplying them with their appropriate duty cycles, as described in Eq. (9) - (12). After the estimation, the obtained matrices of the averaged state space model for the discussed converter are provided in Eq. (13).

$$A = A_1 d_1 + A_3 (d_2 - d_1) + A_4 (1 - d_2) \quad (9)$$

$$B = B_1 d_1 + B_3 (d_2 - d_1) + B_4 (1 - d_2) \quad (10)$$

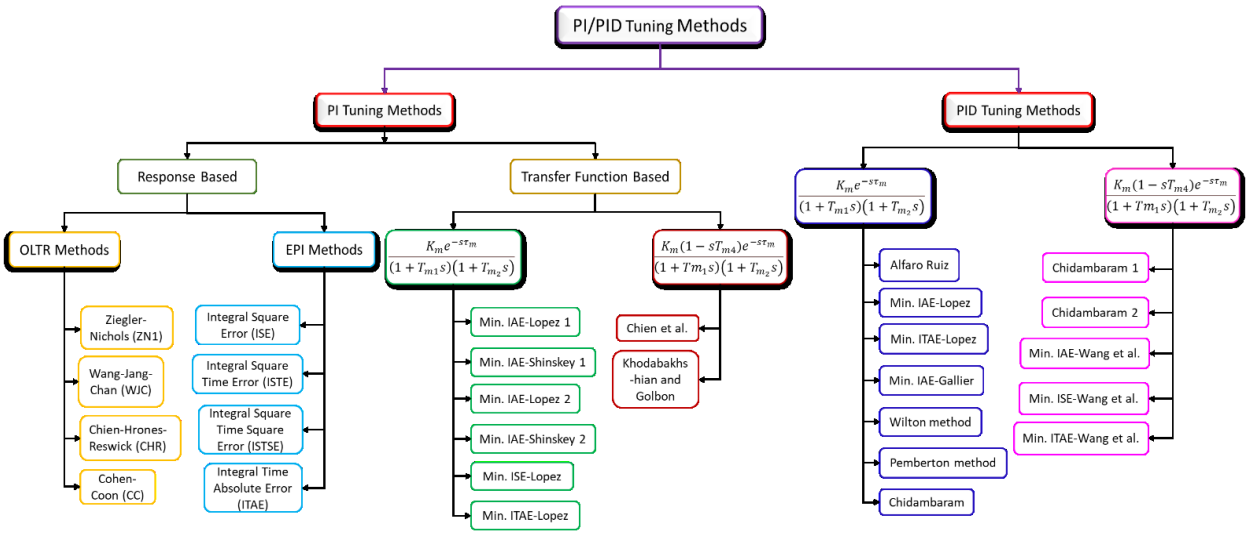

Fig. 5. Various types of PI/PID tuning methods implemented in present work.

$$C = C_1 d_1 + C_3 (d_2 - d_1) + C_4 (1 - d_2) \tag{11}$$

$$D = D_1 d_1 + D_3 (d_2 - d_1) + D_4 (1 - d_2) \tag{12}$$

where,

A_1, B_1, C_1, and D_1 are the state matrices of operating Mode I, A_3, B_3, C_3, and D_3 are the state matrices of operating Mode III and A_4, B_4, C_4, and D_4 are the state matrices of operating Mode IV.

By solving the above equations, the final matrices of the state space averaged method are obtained as described in Eq. (13), this will be used to get the transfer function of the converter. For the purpose of current control, element (1,1) is the appropriate transfer function, and for the voltage control, element (2,2) is considered. This is because the transfer function represented by the diagonal elements of the matrix 'TF' will have a direct impact on the output with respect to the corresponding input.

$$A = \begin{pmatrix} 0 & \frac{-1}{L} \\ \frac{1}{C} & \frac{-1}{R_L C} \end{pmatrix};\ B = \begin{pmatrix} \frac{1}{L} & \frac{1}{L} \\ 0 & 0 \end{pmatrix};\ C = \begin{pmatrix} 1 & 0 \\ 0 & 1 \end{pmatrix};\ D = [0] \tag{13}$$

$$TF = \begin{vmatrix} \frac{i_L}{d_1} & \frac{V_C}{d_1} \\ \frac{i_L}{d_2} & \frac{V_C}{d_2} \end{vmatrix} \tag{14}$$

The design specifications of the converter are $V_1 = 12$ V, $V_2 = 5$ V, $L = 330$ mH, $C = 470$ µF, R_L=10 Ω, and $V_O = 7$ V. The transfer functions represented by the diagonal elements in Eq. (14), are derived and are given in Eq. (15) and Eq. (16). These transfer functions will be used to design the 2-loop control of the DISO converter and are specific to this converter for the considered design specifications.

$$\frac{V_C}{d_2} = \frac{3.224 \times 10^4}{s^2 + 212.8s + 6647} \tag{15}$$

$$\frac{i_L}{d_1} = \frac{36.36s + 7737}{s^2 + 212.8s + 6647} \tag{16}$$

3. Implementation of the PI/PID Controller

The schematic of a two-loop control of the DISO buck converter is shown in Fig.4. The two loops regulate the inductor current i_L and output voltage V_0 of the system. In the outer loop, the output voltage is fed back and compared with the reference voltage, and the error signal is fed as input to the PI/PID controller. This controller adjusts the gains, provides the current reference signal, and generates control input d_2 which is the duty cycle for the switch S_2. The measured inductor current of the converter is given as feedback and is compared with the reference signal that comes from the first PI/PID controller and generates the second error signal. This error signal is fed to the second PI/PID controller to generate control signal d_1 which is the duty cycle for switch S_1. Thus, the two closed loops govern the two state variables.

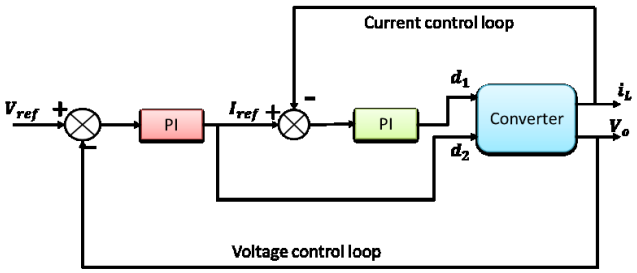

Fig. 4. Block diagram of two-loop control of Dual Input Buck converter.

Numerous PI/PID gain tuning methods are presented in Fig.5. The mathematical equations used to generate control signal $u(t)$ for a PI and PID controllers are given in Eq. (17) and Eq. (18) respectively.

$$u(t) = K_p e_p(t) + K_i \int e_i(t) dt \tag{17}$$

$$u(t) = K_p e_p(t) + K_i \int e_i(t) dt + K_d \frac{d}{dt} e_d(t) \tag{18}$$

where K_p, K_i, and K_d are the gain parameters corresponding to the P, I, and D components of a PID controller. The PI controller gains tuning methods are broadly classified into response-based methods and transfer function based tuning methods. Response based methods are in general applicable to any type of system and should be implemented in open loop configuration. Transfer function based methods are specific to the type of sytem and the gain tuning methods depend on the system gain and response characteristics.

3.1. Response based Tuning Methods

In response-based tuning methods, the gains K_p, and K_i are calculated from the step response of the system. This should be done without incorporating any feedback paths as shown in Fig.6(a).

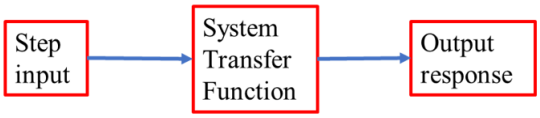

Fig. 6(a). Open Loop Transient Response (OLTR) method.

From the output response, the parameters such as stationary gain (K_s), Slope of a tangent line (M), dead time (T_d), and time constant (τ_c) as depicted in Fig.6(b).

Using the measured values from the step response, the controller gains can be computed. There is a slight difference in the computation of controller gains when different sub-methods such as Ziegler-Nichols (ZN1), Wang-Jang-Chan (WJC), Chien-Hrones-Reswick (CHR), and Cohen-Coon (CC) methods are used. The Transfer function of the converter to design the voltage controller and the transfer function of the converter to design the current controller are given in Eq. (15) & Eq. (16) respectively. The process of finding K_p and K_i values using the error performance index (EPI) method is the same as that used for the OLTR method. Integral Square Error (ISE), Integral Square Time Error (ISTE), Integral Square Time Square Error (ISTSE), and Integral Time Absolute Error (ITAE) methods are some of the ways in which the controller gain parameters are computed. The controller gain values computed for a PI controller using OLTR and EPI methods for both voltage and current regulation and respective values are tabulated in Table 3.

3.2. Transfer Function-based Tuning Methods

Transfer function-based methods compare the transfer function of the system under consideration with the standard transfer functions and thus compute the gain parameters of the PID controller. To implement the two-loop control system, the transfer functions of the two state variables are supplied with step input signal, and PI/PID controller with unity feedback separately as depicted in Fig.7(a) and Fig.7(b).

By looking at the model of the transfer function, the self-regulating process methods presented in [30] can be implemented to estimate the gains of PID controllers. Some of the applicable tuning methods are implemented for both the converter transfer functions and estimated K_p, K_i, and K_d values are tabulated separately in Tables 4 & 5 respectively.

Table 3. PI controller gains for OLTR and EPI methods

Method	Voltage Controller		Current Controller	
	K_p	K_i	K_p	K_i
ZN	9.843	3699.024	0.183	0.356
WJC	71.245	3464.593	0.114	0.0029
CHR	3.828	3955.967	0.0715	0.381
CC	10.03	3932.213	0.0102	-0.027
ISE	3.762	215.425	0.128	0.0039
ISTE	3.740	181.335	0.127	0.0032
ISTSE	3.554	170.449	0.122	0.0032
ITAE	2.977	116.704	0.09	0.0029

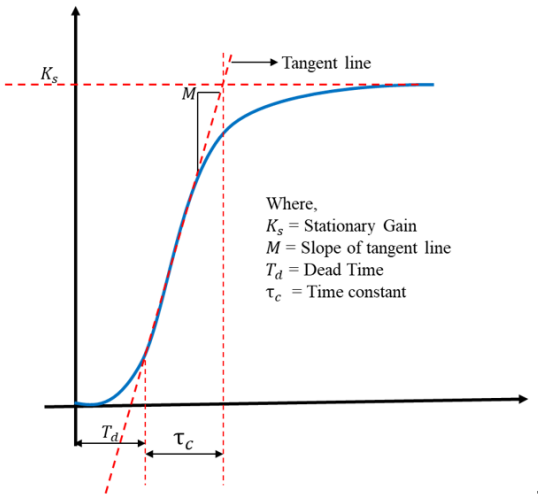

Fig. 6(b). Implementation of OLTR and EPI.

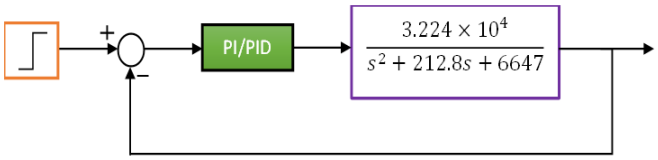

Fig. 7(a). Schematic for Voltage control of the converter.

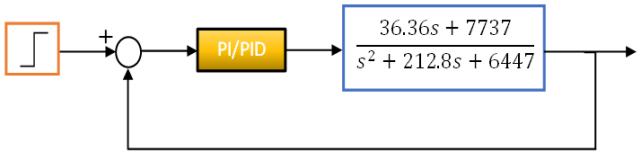

Fig. 7(b). Schematic for Current control of the converter.

4. Performance Analysis of the Designed Controller

To know the performance of the designed controller and the efficiency of the tuning method some performance indices are evaluated in this section. They are time domain analysis and frequency domain analysis. These two are illustrated separately along with their performance indices tables in this section.

Table 4. Transfer function based PID parameters for Voltage controller

S. No.	Method	K_p	K_i	K_d
1.	Min. IAE-Lopez 1	1.94	67.761	-
2.	Min. IAE-Shinskey 1	0.8088	250.7	-
3.	Min. IAE-Lopez 2	3	141.5094	-
4.	Min. IAE-Shinskey 2	4.743	275.8	-
5.	Min. ISE-Lopez 1	4.1	156.8303	-
6.	Min. ITAE-Lopez 1	2.3	123.1692	-
7.	Albaro Ruiz	221.0151	31.382×10^{3}	0.248916
8.	Min. IAE-Lopez 3	7	562.2942	0.0191716
9.	Min. ISE - Lopez 2	7.6	2.9071×10^{3}	0.02365
10.	Min. ITAE-Lopez 2	6.2	498.032	0.013507
11.	IAE 2 (Gallier)	1.34	44.67	1.087×10^{-2}
12.	Wilton 1	0.9798	29.69	4.605×10^{-3}
13.	Wilton 2	0.4243	12.86	1.994×10^{-3}
14.	Van Der Grinten	8.283	248	5.301×10^{-2}
15.	Pemberton	5.4555	165.3182	1160.7447
16.	Chidambaram	0.3269	4.5152	31.7379

Table 5. Transfer function based PID parameters for the Current controller

S. No.	Method	K_p	K_i	K_d
1.	Chien et al	0.1307	4.785	-
2.	Khodabakhshian & Golbon	8.246	1.115×10^{2}	-
3.	Chidambaram 1	0.4398	13.33	2.067×10^{-3}
4.	Chidambaram 2	2.636×10^{-2}	0.3641	2.718×10^{-4}
5.	Min. IAE-Wang	11.98	128.5	0.1283
6.	Min. ISE-Wang	8.203	88.02	8.589×10^{-2}
7.	Mn. ITAE-Wang	11.69	125.4	0.1252

4.1. Time Response Analysis

Variation of the output response to time is known as Time domain Response. Time response indices are Peak Time (T_p), Rise Time (T_r), Settling Time (T_s), and Percentage Overshoot (%OS). Practically the output response consists of a Transient period and steady state period. By evaluating these time response indices, one can know how much time the system is taking to reach the steady state. Here, the lesser the transient period indicates that the system will reach the desired output more quickly, and is efficient. The time response parameters are computed for voltage control of a DISO converter using the K_p, K_i, and K_d parameters from Tables 3 – 4 and are given in Table 6. From Table. 6, it can be noted that among OLTR methods, only the WJC method has provided the time response parameters whereas the PID parameters computed using other OLTR methods have not provided a stable output. The response of the DISO converter with K_p, K_i, and K_d parameters computed using OLTR methods is given in Fig.8(a) and Fig.8(b). The response with parameters computed using the EPI methods is depicted in Fig. 9.

Table 6. Calculated time response parameters for Voltage control

S. No.	Method	T_p	T_r	T_s	%OS
Open Loop Transient Response-based methods					
1.	ZN-1	*Unstable*			
2.	WJC	1.002	0.001	1.042	82.1
3.	CHR	*Unstable*			
4.	CC	*Unstable*			
Error Performance Index-based Methods					
5.	ISE	1.009	0.004	1.041	50.6
6.	ISTE	1.009	0.004	1.041	47.5
7.	ISTSE	1.009	0.004	1.042	45.7
8.	ITAE	1.011	0.005	1.043	39.1
Transfer Function-based Methods					
9.	Min. IAE-Lopez 1	1.013	0.006	1.034	29.7
10.	Min. IAE-Shinskey 1	*Unstable*			
11.	Min. IAE-Lopez 2	1.011	0.005	1.045	43.5
12.	Min. IAE-Shinskey 2	1.008	0.003	1.048	54.9
13.	Min. ISE-Lopez 1	1.008	0.004	1.039	45.4
14.	Min. ITAE-Lopez 1	1.013	0.005	1.048	40.2
15.	Albaro Ruiz	1.001	0.001	1.083	95
16.	Min. IAE-Lopez 3	1.006	0.002	1.038	61.6

17.	Min. ISE - Lopez 2	*Unstable*			
18.	Min. ITAE-Lopez 2	1.007	0.002	1.041	60.6
19.	IAE 2	1.012	0.005	1.031	14.2
20.	Wilton 1	1.016	0.009	1.041	6.5
21.	Wilton 2	0	0.028	1.07	0
22.	Van Der Grinten	1.005	0.002	1.03	54.7
23.	Pemberton	*Unstable*			
24.	Chidambaram	1	0	1.025	95.2

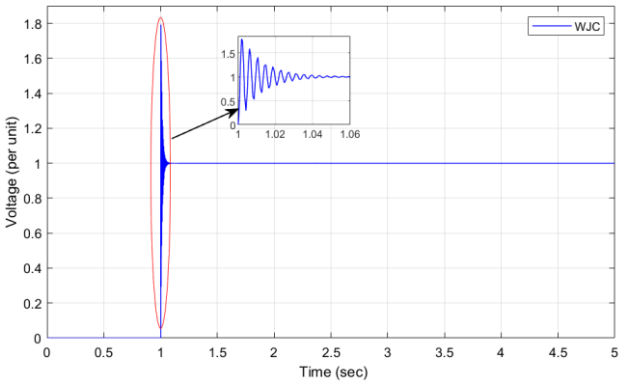

Fig. 8(a). Output response of voltage controller with WJC method.

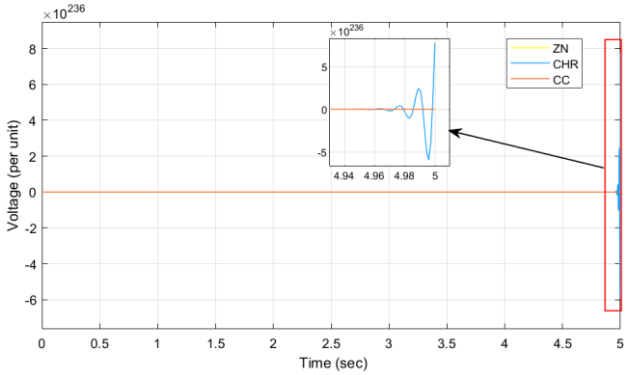

Fig. 8(b). Output response of voltage controller with ZN-CHR-CC methods.

The response of the closed loop DISO converter with PI gain parameters computed using transfer function based tuning methods in Fig.10. Among the 6 PI tuning methods, the Min IAE-Shinsky 1 tuning method has not provided a stable output. Fig. 11. illustrates the output response of transfer function based PID tuning methods, Min. ISE-Lopez 2 & Pemberton methods do not provide stable response.

Table 7. shows the time response indices for the current control of the DISO converter. The PID controller parameters are computed using different tuning methods and these values are used in closed-loop control to compute the time response indicators.

The illustrations of the step response obtained by using the PID parameters computed by OLTR methods for current control are depicted in Fig.12. The illustrations for the response obtained using EPI methods are depicted in Fig.13. The responses for transfer function based tuning methods with PI controller are depicted in Fig.14, and the responses with PID controller are depicted in Fig.15.

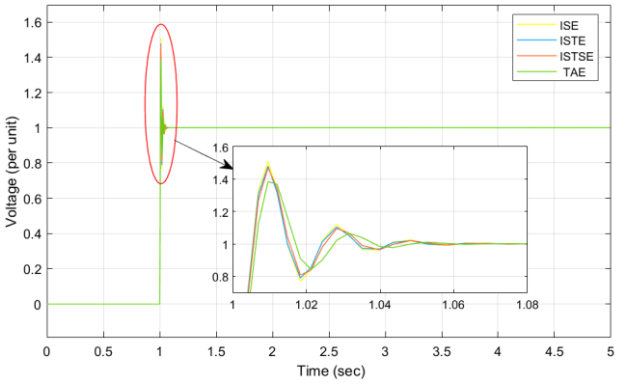

Fig. 9. Output Response of voltage controller with EPI methods.

Table 7. Time response parameters for current control

S. No.	Method	T_p	T_r	T_s	%OS
Open Loop Transient Response-based methods					
1.	ZN-1	1.544	0.203	2.469	14.5
2.	WJC	7.296	0.531	1.958	0
3.	CHR	1.695	0.277	3.07	39.5
4.	CC	*Unstable*			
Error Performance-Based Methods					
5.	ISE	-	0.479	1.849	0
6.	ISTE	-	0.481	1.865	0
7.	ISTSE	-	0.497	1.891	0
8.	ITAE	-	0.67	2.193	0
Transfer Function-based Methods					
9.	Chien et al	1.217	0.08	2.502	59.8
10.	Khodabakhshian & Golbon	1.021	1.007	1.068	3.6
11.	Chidambaram 1	1.121	0.048	1.489	36.7
12.	Chidambaram 2	1.798	0.301	8.202	66.7
13.	Min. IAE-Wang	1.062	0.002	1.015	1.2
14.	Min. ISE-Wang	1.074	0.005	1.018	1.8
15.	Mn. ITAE-Wang	1.073	0.003	1.015	1.3

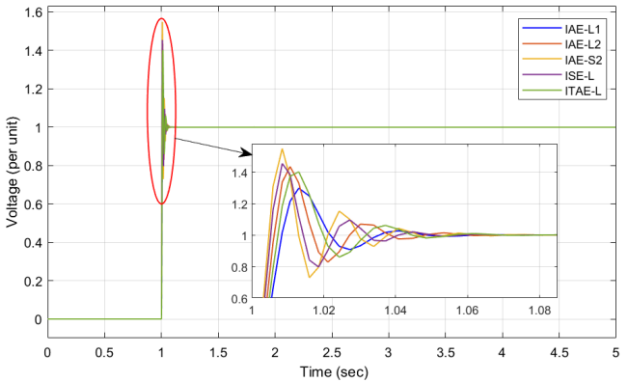

Fig. 10. Output Response of voltage controller with Transfer Function based methods (PI).

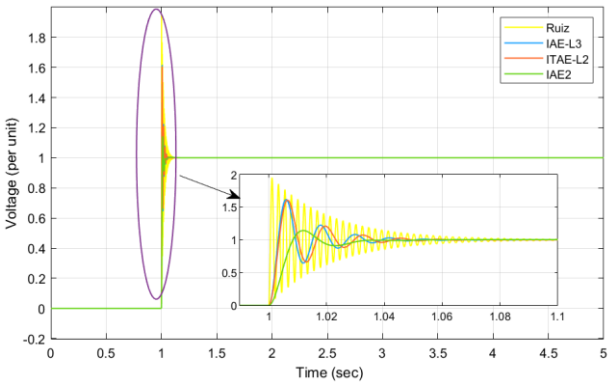

Fig. 11(a). Output Response of voltage controller with Transfer Function based methods (PID).

4.2. Frequency Response Analysis

The frequency response of the system is the combination of magnitude and phase responses. These plots can be drawn separately. The magnitude plot is drawn in dB (decibels) with respect to the frequency, and the phase plot is drawn in degrees (angle) with respect to the frequency on the imaginary axis. If these plots were drawn as a function of log ω such plots are called Bode Plots. From these plots, one can analyze the stability of the system to be controlled.

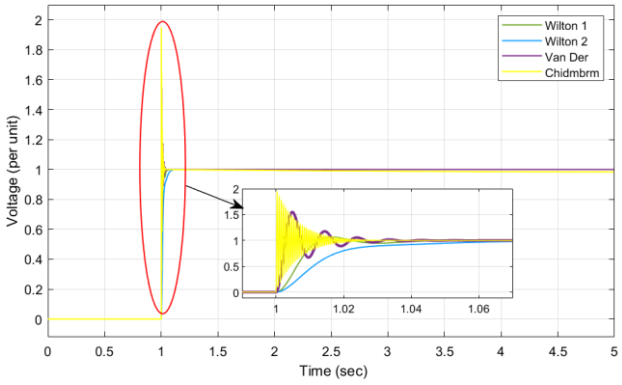

Fig. 11(b). Output Response of voltage controller with Transfer Function based methods (PID).

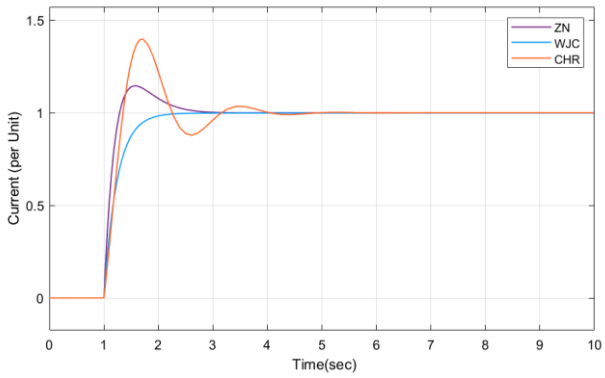

Fig. 12. Output response of current controller with OLTR tuning methods.

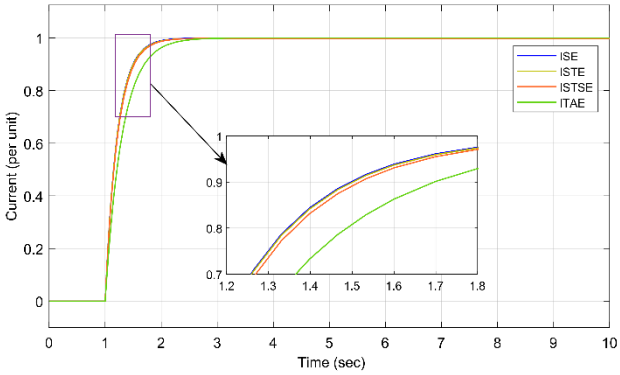

Fig. 13. Output response of current controller with EPI tuning methods.

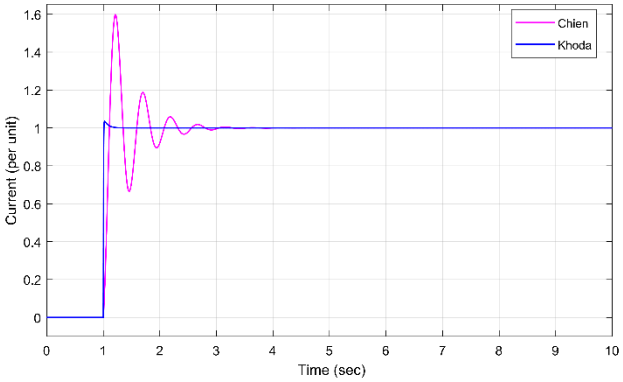

Fig. 14. Output response of current controller with Transfer Function-based PI tuning method.

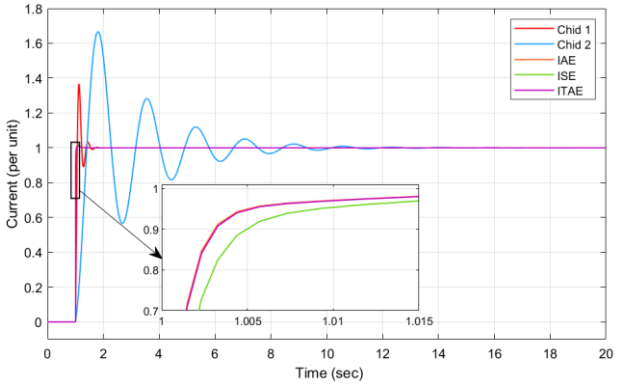

Fig. 15. Output response of current controller with Transfer function-based PID tuning methods.

The bode plots are drawn for all the mentioned tuning methods and calculated for the Phase Margin and the status of the stability. The Gain Margin for the considered transfer functions was not determined because the transfer function already has a high gain so the phase curve does not exceed 180 degrees. The frequency response parameters for the DISO converter voltage controller are tabulated in Table. 8 and Table. 9 gives the frequency response parameters for the current controller. The frequency responses of the DISO converter with voltage controller are shown in Fig.16 – Fig.18. The illustrations of the frequency response with OLTR tuning methods and EPI tuning methods are depicted in Fig.16 & Fig.17 respectively. In which the WJC method is showing a stable response in OLTR methods and all the EPI methods are showing stable response. Fig. 18. illustrates the frequency responses with Transfer function-based tuning methods for PI & PID controllers. Among all the tuning methods of voltage controller, the transfer function based tuning methods with PID controller show the highest stability such as Van Der Grinten, IAE 2, and Wilton 1.

Table 8. Frequency response parameters for the Voltage controller

S.No.	Method	Phase Margin (deg)	Stability
1	ZN-1	-19.9	No
2	WJC	8.78	Yes
3	CHR	-80	No
4	CC	-21.6	No
5	ISE	36.4	Yes
6	ISTE	38.9	Yes
7	ISTSE	40	Yes
8	ITAE	46.6	Yes
9	Min. IAE-Lopez 1	60.5	Yes
10	Min. IAE-Shinskey 1	-15.6	No
11	Min. IAE-Lopez 2	43.9	Yes
12	Min. IAE-Shinskey 2	32.2	Yes
13	Min. ISE-Lopez 1	39.7	Yes
14	Min. ITAE-Lopez 1	48.1	Yes
15	Albaro Ruiz	2.74	Yes
16	Min. IAE-Lopez 3	26	Yes
17	Min. ISE - Lopez 2	-7.06	No
18	Min. ITAE-Lopez 2	27.2	Yes
19	IAE2	**156**	Yes
		79.8	
20	Wilton 1	136	Yes
		113	
21	Wilton 2	Indeterminant	No
22	Van Der Grinten	**177**	Yes
		29.1	
23	Pemberton	0.414	Yes
24	Chidambaram	2.51	Yes

Table 9. Frequency response parameters for the Current controller

S.No.	Method	Phase Margin (deg)	Stability
1.	ZN-1	139	Yes
2.	WJC	Indeterminant	No
3.	CHR	89.8	Yes
4.	CC	Indeterminant	No
5.	ISE	Indeterminant	No
6.	ISTE	Indeterminant	No
7.	ISTSE	Indeterminant	No
8.	ITAE	Indeterminant	No
9.	Chien et al	54.2	Yes
10.	Khodabakhshian & Golbon	163	Yes
11.	Chidambaram 1	97.4	Yes
12.	Chidambaram 2	42	Yes
13.	Min. IAE-Wang	**176**	Yes
14.	Min. ISE-Wang	**175**	Yes
15.	Mn. ITAE-Wang	**176**	Yes

The frequency responses of the DISO converter with voltage controller are shown in Fig.16 – Fig.18. The illustrations of the frequency response with OLTR tuning methods and EPI tuning methods are depicted in Fig.16 & Fig.17 respectively. In which the WJC method is showing a stable response in OLTR methods and all the EPI methods are showing stable response. Fig. 18. illustrates the frequency responses with Transfer function-based tuning methods for PI & PID controllers. Among all the tuning methods of voltage controller, the transfer function based tuning methods with PID controller show the highest stability such as Van Der Grinten, IAE 2, and Wilton 1. Figures 19 – 21 illustrate the frequency responses of the DISO converter with the current controller. Among all the response based tuning methods only ZN-1 and CHR methods showed the stable frequency response (Fig.19 & 20). The frequency responses of the

transfer function-based methods are illustrated in Fig.21 separately for PI and PID controllers.

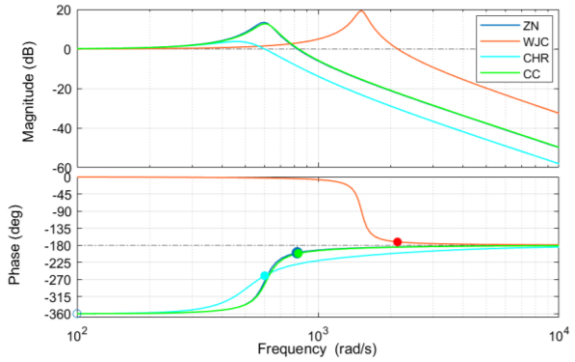

Fig. 16. Frequency response of voltage controller with OLTR methods.

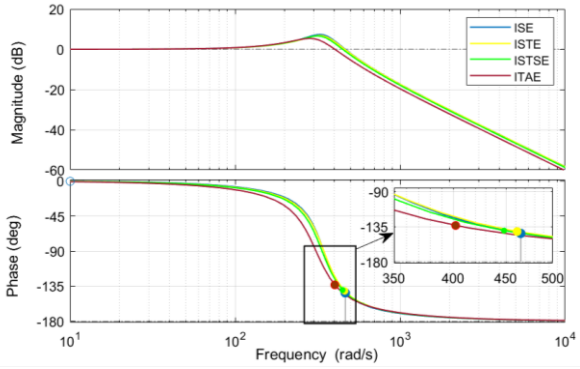

Fig. 17. Frequency responses of Voltage controller with EPI methods.

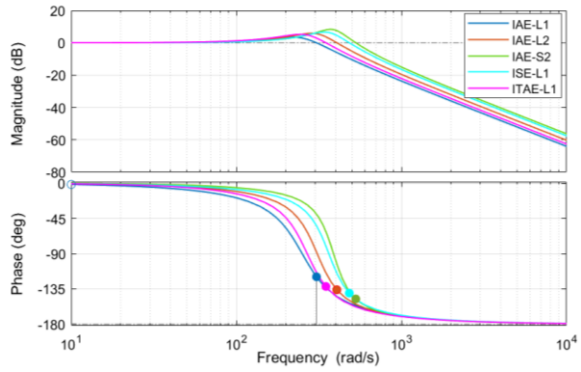

Fig. 18(a). PI Controller methods.

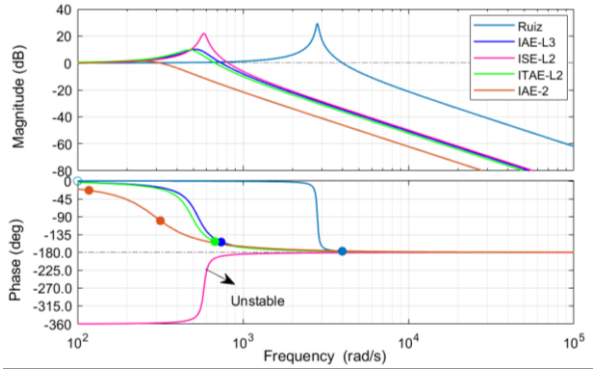

Fig. 18(b). PID Controller methods.

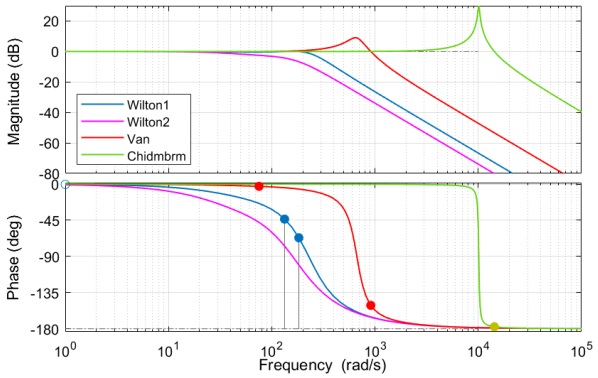

Fig. 18(c). PID Controller methods

Fig. 18. Frequency responses of voltage controller with the Transfer function-based tuning methods.

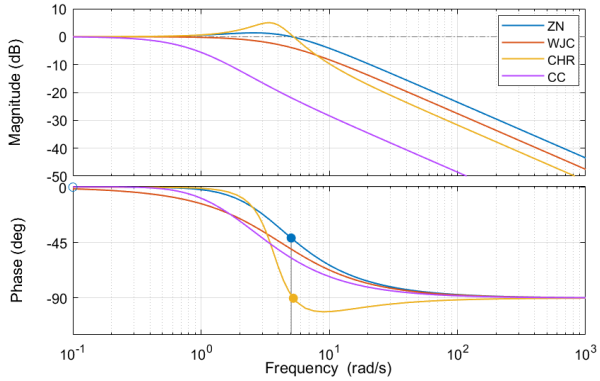

Fig. 19. Frequency responses of Current controller with OLTR methods.

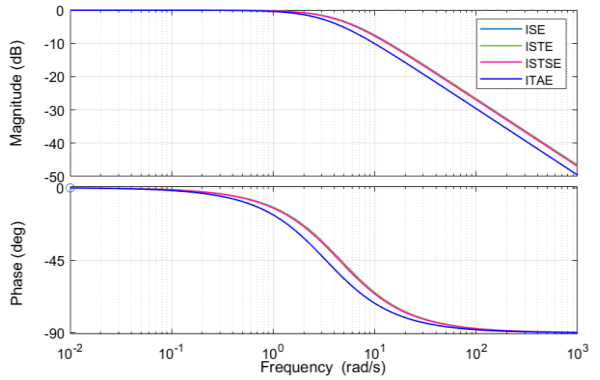

Fig. 20. Frequency responses of Current controller with EPI methods.

Among all the tuning methods that are implemented for the current controller, IAE-Wang, ITAE-Wang, and ISE-Wang show the highest stable responses than others.

5. Summary of Results

In this section, the best tuning methods are nominated based on the following assumptions. The lower the PID controller gain, the better the tuning method, since higher gain values lead to increased hardware implementation costs. From the time response parameters, the best tuning method requires the peak overshoot to be low, as higher peak overshoots may result in hardware damage. The rise time and settling time

parameters are important parameters that give us information regarding the response time of the converter and also how long the converter takes to settle.

Typically, these values should be lower. From the frequency response analysis, the gain margin and phase margin are derived. All the frequency response based tuning methods have resulted in a very high gain margin. So, phase margin is considered to discuss the stability of the converter. The larger the phase margin, the better the stability. In Tables 10 and 11, the time domain parameters (Rise time, Settling time, and %Overshoot) and frequency domain parameters (phase margin) of a DISO voltage controller and current controller are presented.

Table 10. Summary of best tuning methods for Voltage controller

Parameter / Tuning methods	Phase Margin	T_r	T_s	%OS
Van Der Grinten	177	0.002	1.03	54.7
IAE 2	156	0.005	1.031	14.2
WJC	8.78	0.001	1.042	79.2
Albaro Ruiz	2.74	0.001	1.083	95
Chidambaram	2.51	0	1.025	95.2
Wilton 2	Not Stable	0.028	1.07	0

Table 11. Summary of best tuning methods for Current controller

Parameter / Tuning methods	Phase Margin	T_r	T_s	%OS
Min. IAE-Wang	176	0.002	1.015	1.2
Min. ITAE-Wang	176	0.003	1.015	1.3
WJC	Not Stable	0.531	1.95	0
ISE	Not Stable	0.479	1.849	0
ISTE	Not Stable	0.481	1.865	0
ISTSE	Not Stable	0.497	1.891	0
ITAE	Not Stable	0.67	2.193	0

6. Conclusion

The present work aims to design an efficient two-loop PI/PID controller for a dual input single output buck (DISO) converter. The tuning methods to compute gains of P, I, and D controllers to control the output voltage of the DISO converter by implementing voltage and current control loops

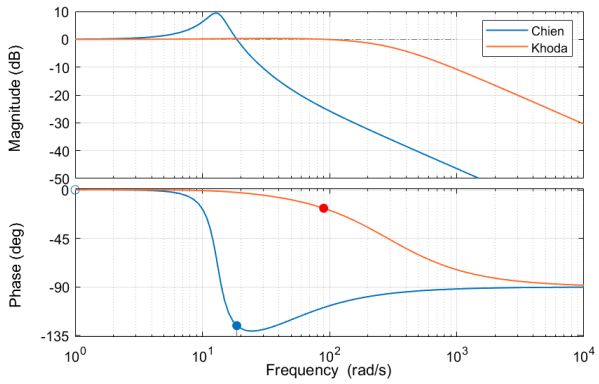

Fig. 21(a). PI Controller methods.

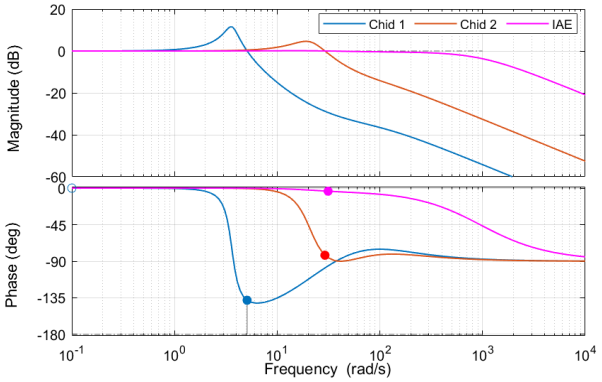

Fig. 21(b). PID Controller methods.

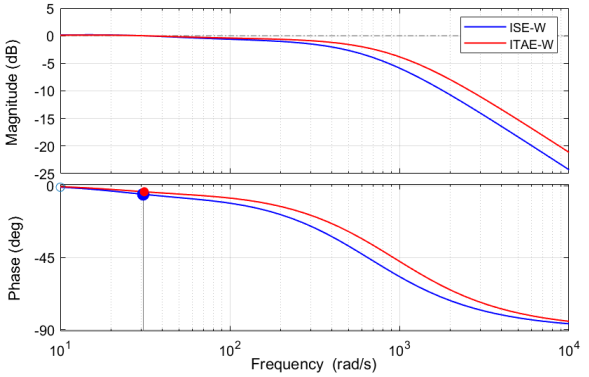

Fig. 21(c). PID Controller methods.

Fig. 21. Frequency responses of Current controller with transfer function-based methods.

are presented. Response-based (OLTR and EPI) and transfer function-based, tuning methods are implemented for both voltage control and current control. The efficacy of the implemented methods is evaluated by computing time domain and frequency domain performance indices.

Assuming the controller gain as the performance metric, the ITAE method is preferred as it offers lower gain values with the PI combination. Wilton 2 tuning method has provided a lower gain solution when the converter is controlled with a PID controller for the voltage control loop and Chidambaram 2 tuning method offered a better gain for the current control loop.

From the time response parameters, the Wilton 2 tuning method has provided a lower peak overshoot and lower peak time. And Chidambaram tuning method provided a lower rise time and lower settling time. Thus, both methods can be considered as superior for voltage controller. For the current controller, all the EPI methods have provided the best performance in terms of peak time and peak overshoot. The tuning method IAE – Wang has resulted in a lesser rise time and lesser settling time. Thus, EPI methods and IAE – Wang method can be considered as the superior.

From the frequency response analysis, the Van Der Grinten method shows superior performance in the case of a voltage controller. IAE – Wang and ITAE – Wang methods gave the highest and equal phase margin value in the case of a current controller.

The performance of the tuning methods when analyzed by considering all or a combination of the time and frequency domain parameters, gives a different view when compared to analyzing the performance concerning individual parameters.

In the case of a DISO converter, the peak overshoot is considered an important parameter. If the converter is improperly handled with high overshoot, it can physically damage the converter. For DISO current controller, 1.2% of peak overshoot is reported for IAE – Wang and ITAE – Wang methods of PID tuning. Also, the phase margin of 176^0 is computed which gives us the information that these methods provide low peak overshoot with high stability. In the case of the voltage controller, a peak overshoot difference of 81% is observed between the best and the worst PID tuning method along with a phase margin of 156^0. This is observed when the voltage controller is tuned with the IAE-2 method.

Author Contributions

Sarala Kumari Gurijala was responsible for software development, data curation, original draft Preparation, visualization, John Pradeep Darsy was responsible for the validation, resources, review and editing, project administration, and supervision. Both the authors jointly contributed to the conceptualization, methodology, formal analysis, investigation. All authors have read and agreed to the published version of the manuscript.

Conflict of Interest

The author(s) declared no potential conflicts of interest with respect to the research, authorship, and/or publication of this article.

References

[1] M.Y. Ali Khan, L. Saeed, S. H. Khan, and J. Saleem, “Design of a multi-input single-output DC-DC boost converter for micro grid application,” International Conference on Engineering and Emerging Technologies (ICEET), Lahore, Pakistan, 2019, pp. 1–6.

[2] S.R. Khasim and C. Dhanamjayulu, “Selection parameters and synthesis of multi-input converters for electric vehicles: An overview,” Renewable and Sustainable Energy Reviews, vol. 141, p. 110804, 2021.

[3] M. Gavriş, O. Cornea, and N. Muntean, “Multiple input DC-DC topologies in renewable energy systems – A general review,” 3rd International Symposium on Exploitation of Renewable Energy Sources, Subotica, Serbia, Mar. 11–12, 2011.

[4] B. Karthikeyan, K. Sundararaju, R. Palanisamy, R. Manivasagam, I. Hossain, M. Bajaj, M. Shouran, B. A. Samad, and S. Kamel, “A dual input single output non-isolated DC-DC converter for multiple sources electric vehicle applications,” Frontiers in Energy Research, vol. 10, p. 979539, 2022.

[5] Y.M. Chen, Y.C. Liu, and S.H. Lin, “Double-input PWM DC/DC converter for high-/low-voltage sources,” IEEE Transactions on Industrial Electronics, vol. 53, no. 5, pp. 1538–1545, Oct. 2006.

[6] A.H. Chander, L. K. Sahu, S. Ghosh, and K. K. Gupta, “Comparative analysis on selection and synthesis of multiple input converters: A review,” IET Power Electronics, vol. 13, pp. 611–626, 2020.

[7] V.A.K. Prabhala, M. Khazraei, and M. Ferdowsi, “A new control strategy for a class of multiple-input DC-DC converters,” International Conference on Renewable Energy Research and Application (ICRERA), Milwaukee, WI, USA, 2014, pp. 508–513.

[8] A. Sahbani, K. Cherif, and K. Ben Saad, “Multiphase interleaved bidirectional DC-DC converter for electric vehicles and smart grid applications,” International Journal of Smart Grid, vol. 4, no. 2, Jun. 2020.

[9] L. Larbi, S. Hadji, A. Belkaid, I. Çolak, and R. Bayindir, “Design of a buck converter battery charging controller in PV plant,” 10th International Conference on Smart Grid (icSmartGrid), Istanbul, Turkey, 2022, pp. 214–220.

[10] F. Issi and O. Kaplan, “Simulation of wireless charging multiple e-scooters using PV array with class-E inverter fed by PI controlled boost converter for constant output voltage,” 10th International Conference on Smart Grid (icSmartGrid), Istanbul, Turkey, 2022, pp. 61–65.

[11] Y. Furukawa, Y. Shibata, T. Suetsugu, I. Çolak, and F. Kurokawa, “Digital peak current mode control DC-DC converter for renewable energy system,” 11th International Conference on Renewable Energy Research and Application (ICRERA), Istanbul, Turkey, 2022, pp. 485–489.

[12] S. Bairabathina and S. Balamurugan, “Modelling and real-time validation of a two-input high-gain DC-DC converter with a reduced number of switches,” International Journal of Renewable Energy Research, vol. 13, no. 3, Sep. 2023.

[13] M. Alzgool and H. Nouri, “PID controller design for a novel multi-input multi-output boost converter hub,” JEA Journal of Electrical Engineering, vol. 2, no. 1, 2018.

[14] V.B. Kumar, G. Charan, and Y.V.P. Kumar, "Design of Robust PID controller for improving voltage response of a Cuk converter," in Innovations in Electrical and Electronic Engineering, Lecture Notes in Electrical Engineering, vol. 661, Springer, Singapore, 2021.

[15] S.B. Prusty, S. Padhee, U.C. Pati, and K.K. Mahapatra, "Comparative performance analysis of various tuning methods in the design of PID controller," Michael Faraday IET International Summit (MFIIS), Kolkata, India, Sep. 12–13, 2015.

[16] K.S. Rao, D.J. Pradeep, Y.V.P. Kumar; M.K. Chakravarthi, Ch.P. Reddy, "Quantitative analysis on open-loop PI tuning methods for liquid level control," 4th International Symposium on Advanced Electrical and Communication Technologies (ISAECT), Dec. 2021.

[17] V.B. Kumar, D. Sampath, V.N.S. Praneeth, and Y.V.P. Kumar, "Error performance index based PID tuning methods for temperature control of heat exchanger system," IEEE International IOT, Electronics and Mechatronics Conference (IEMTRONICS), 2021.

[18] K. Ramireddy, Y. Hirpara, and Y.V.P. Kumar, "Transient performance analysis of buck-boost converter using various PID gain tuning methods," 12th International Conference on Computational Intelligence and Communication Networks (CICN), Bhimtal, India, 2020, pp. 321–326.

[19] K.V.P. Srikar, Y.V.P. Kumar, D.J. Pradeep, and C.P. Reddy, "Investigation on PID controller tuning methods for aircraft fuselage temperature control," International Symposium on Advanced Electrical and Communication Technologies (ISAECT), Marrakech, Morocco, 2020, pp. 1–5.

[20] R. Karthik, A. S. Hari, Y. V. P. Kumar, and D. J. Pradeep, "Modelling and control design for variable speed wind turbine energy system," International Conference on Artificial Intelligence and Signal Processing (AISP), Amaravati, India, 2020, pp. 1–6.

[21] A.K. Aseem and S.K. Selva Kumar, "Closed loop control of DC-DC converters using PID and FOPID controllers," International Journal of Power Electronics and Drive System, vol. 11, no. 3, pp. 1323–1332, Sep. 2020.

[22] V.B. Kumar, K.S. Rao, G. Charan, and Y.V.P. Kumar, "Industrial heating furnace temperature control system design through fuzzy-PID controller," IEEE International IOT, Electronics and Mechatronics Conference (IEMTRONICS), Toronto, Canada, 2021, pp. 1–6.

[23] P. Gunawardena and D. Nayanasiri, "A dual-input single-output DC-DC converter topology for renewable energy applications," IEEE Transactions on Industry Applications, vol. 59, no. 2, Mar.–Apr. 2023.

[24] O. Balapanuru, M.M. Lokhande, M.V. Aware, S. Gupta, and F.P.G. Marquez, "Unsymmetrical dual-input isolated high gain bidirectional DC-DC converter with inherent current sharing for light EV applications," IEEE Transactions on Transportation Electrification, 2023.

[25] M. Dhananjaya, S. Pattnaik, D. Potnuru, R. Devarapalli, and F.P.G. Marquez, "Design and analysis of a switch fault-tolerant multi-input single-output DC-DC converter for high reliability applications," International Journal of Electrical Power & Energy Systems, vol. 157, p. 109800, 2024.

[26] C. Li, H. Li, L. Cheng, X. Sun, N. Wang, and W. Li, "A novel non-isolated dual-input single-output high step-up DC/DC converter with coupled inductors," IEEE Transactions on Power Electronics, vol. 38, no. 9, Sep. 2023.

[27] A. Jaswanth, D.S.V Saravana, V.B. Kumar, Y.V.P. Kumar, D.J. Pradeep, C.P. Reddy, "Classical PID based speed control of DC machines with voltage controlled DC/DC converter," in Control Applications in Modern Power Systems, Lecture Notes in Electrical Engineering, vol. 974, Springer, 2023.

[28] A.S. Vidya, V.B. Kumar, Y.V.P. Kumar, D. John Pradeep, C.P. Reddy, "Design of automatic load frequency control loop using classical PID control methods," in Control Applications in Modern Power Systems, Lecture Notes in Electrical Engineering, vol. 974, Springer, 2023.

[29] L.P.S.S. Pallavi, V.B. Kumar, Y.V.P. Kumar, D.J. Pradeep, C.P. Reddy, "Design of automatic voltage regulator loop using classical PID control methods," in Control Applications in Modern Power Systems, Lecture Notes in Electrical Engineering, vol. 974, Springer, 2023.

[30] A. O'Dwyer, Handbook of PI and PID Controller Tuning Rules, 3rd ed., London: Imperial College Press, 2009.

[31] J. Reddy and N. Sudhakar, "Energy sources and multi-input DC-DC converters used in hybrid electric vehicle applications – A review," International Journal of Hydrogen Energy, vol. 43, no. 36, pp. 17387–17408, 2018.

[32] M. Hichem, B. Tahar, B. Aziz, and D. Djalel, "Study and analysis of the operation of a Cuk converter for precise voltage regulation," International Journal of Smart Grid, vol. 7, no. 3, Sep. 2023.

[33] K.P. Yalamanchili, M. Ferdowsi, and K. Corzine, "New double input DC-DC converters for automotive applications," IEEE Vehicle Power and Propulsion Conference (VPPC), Windsor, UK, 2006, pp. 1–6.